RSC Advances

ROYAL SOCIETY OF CHEMISTRY

www.rsc.org/advances

Effects of different functional groups on metastatic behaviors of SPC-A-1/human lung cancer cells in self-assembled monolayers

Guan Zheng,[#a,b] Lihua Li,[#b] Mei Li,[b] Xinglong Feng,[b] Xiaobing Pu,[b] Baoliang Zhang,[a,b] Peng Yu,[c] Guanping He,[a] Yu Zhang,[b] Hong Xia* [a,b]

Cancer cell processes and the tumor microenvironment play key roles in metastasis, which is the primary cause of death from lung cancer. We utilized self-assembled monolayers terminated with different functional groups (-CH_3, -OH, -COOH, -NH_2, -SH) to explore their effects on the metastatic behaviors of human lung cancer cells (SPC-A-1) *in vitro*. Cell adhesion was investigated by scanning electron microscopy and 4, 6-diamidino-2-phenylindole staining; rhodamine-phalloidin was further used to directly label microfilaments. Viability/cytotoxicity staining and lactate dehydrogenase assays were performed to determine cell toxicity, and apoptosis was investigated by flow cytometry. Transwell assays were used to analyze the relationship between cell migration and surface chemistry. Genes expression associated with metastatic behaviors was measured by quantitative real-time PCR. Our results demonstrated that -NH_2 and -COOH groups promote adhesion and spreading. Although the -OH group did not affect cell survival and mobility, -CH_3 and -SH groups were toxic to SPC-A-1 cells after 24h of incubation. Furthermore, the -SH group inhibited cell migration and increased gene expression of E-cadherin. The addition of -SH group has a potential application in new biomaterials or drugs for lung cancer metastasis therapy.

1. Introduction

Lung cancer is the most common cause of death from cancer in both men and women, accounting for approximately 28% of all cancer deaths in America and nearly 2.4 million years of life lost in 2010.[1] Although surgical resection and chemotherapy can be successful in some patients, the long-term prognosis for patients is poor because of tumor metastasis, especially in the brain and bones, which represents the primary cause of death from lung cancer and is responsible for 90% of all morbidity.[2] Therefore, improved treatment largely depend on interrupting the metastatic process, which is also the direction of basic tumor research.[3-6] However, understanding the complexity of the mechanisms by which metastasis occurs is daunting. The metastatic process is classically simplified into an orderly sequence of basic steps: local invasion, intravasation, survival in the circulation, extravasation and colonization. This sequence has helped to rationalize the complex set of biological properties that must be acquired for lung cancer to progress toward overt metastatic disease.[7] All these steps are supported by the functions of cancer cells themselves and their microenvironment.[3, 7, 8]

Self-assembled monolayers (SAMs) are widely used as a model surface to explore the effect of surface chemistry on cell functions.[9-13] Functional group-terminated surfaces have been demonstrated to affect metastatic behaviors such as cell morphology, adhesion, proliferation and migration in hepatoma cells (HepG2s), MCF-7 breast cancer cells and human osteosarcoma cells.[14-16] These reports demonstrated that different functional groups have different effects on cancer cells.

Nonetheless, the effects of different functional groups on the metastatic behaviors of SPC-A-1/human lung cancer cells in SAMs remain to be elucidated. Various chemically modified surfaces were prepared with typical functional groups including methyl (-CH_3), hydroxyl (-OH), carboxyl (-COOH), amino (-NH_2) and mercapto (-SH) groups. Cell morphology, adhesion, toxicity, apoptosis and migration were then examined to characterize the effects of these surfaces on SPC-A-1 cells *in vitro*, which is necessary for a better understanding of cell-biomaterial interactions in the tumor microenvironment. The ultimate goal of our study is to design appropriate biomaterials or drugs to reduce the incidence of metastasis in lung cancer.

2. Materials and methods

2.1. Preparation of self-assembled monolayers (SAMs) on Au surfaces

Au surfaces (thickness of ~40 nm) were prepared on glass coverslips by ion beam sputtering (IBS) technique with a Ti layer (thickness of ~10 nm) as a buffer. The wafers were rinsed with ethyl alcohol and triple-distilled water and cleaned with a highly acidic piranha solution (7:3 (v:v) H_2SO_4:H_2O_2) for 10 min.[17] The wafers were washed with ethyl alcohol in an ultrasonic bath for 10 min and then exposed to ultraviolet rays for 30 min. Finally, the Au substrates were immersed in an ethanol solution containing 1 mM 11-mercapto-1-undecane (-OH, Sigma, St. Louis, MO, USA), 12-mercaptododecanoic acid (-COOH, Sigma), 11-amino-1-undecanethiol hydrochloride (-NH_2, Sigma), 1-dodecanethiol (-CH_3, Sigma), or 11-undecanedithiol (-SH, Sigma) for 4 h at room temperature (25°C).

2.2. Substrate characterization

Model surfaces were characterized by contact angle measurements. Ambient air-water substrate contact angle measurements (1 μL ultra-pure H_2O) were obtained using the contact angle system OCA15 (Dataphysics, Filderstadt, Germany) fitted with a digital camera and then analyzed using in-house image analysis software.

2.3. Cell culture

SPC-A-1 cells (ATCC, Manassas, VA, USA) were cultured at 37°C under a 5% CO_2 atmosphere in RPMI 1640 Medium (Gibco, Grand Island, NY, USA) supplemented with 10% fetal bovine serum (FBS, HyClone, Smithfield, Australia). The medium was changed every 48 h.

2.4. Cell adhesion

Scanning electron microscopy (SEM). For cell morphology observations on various SAM-modified surfaces, cells were seeded on modified surfaces at a density of 6×10^3 cell/cm^2 for 24 h and fixed with 3% glutaraldehyde for 5 h at 4°C. The cells were washed three times with PBS, treated with a graded series of ethanol (50%, 70%, 95% and 100%) at each concentration twice for 10 min each, then dewatered with acetone and isoamyl acetate, followed by air drying in a fume hood. After being sputter-coated with gold, the samples were observed with a scanning electron microscope (SEM, ZEISS Ultra 55, Jena, Germany) at an accelerating voltage of 15 kV.

Cytoskeleton distribution. Adherent cells on SAMs were fixed with 3.7% paraformaldehyde for 15 min, permeabilized in 0.1% buffered Triton X-100 (Sigma) for 5 min, and incubated with PBS-1% BSA (bovine serum albumin) for another 30 min at room temperature. Cell cytoskeletal filamentous actin (F-actin) was stained with ActinRed (Keygentec, Nanjing, China) for 20 min and rinsed with PBS twice, and the cells were then counterstained with 4',6-diamidino-2-phenylindole (DAPI, Roche, Berlin, Germany). The immunostained cells were visualized with a fluorescent microscope (Olympus, BX51).

DAPI staining. After incubation with the cells for 30, 60 and 90 min, the SAMs were rinsed three times with PBS. Next, the adherent cells were fixed with 4% paraformaldehyde and stained with the nuclear stain DAPI. Cell adherence was determined by counting five different areas per sample using a fluorescence microscope (Olympus, BX51) at a magnification of 100×, and the results are expressed as the number of adherent SPC-A-1 in five random fields. The samples were analyzed in triplicate.

2.5. Cell migration assays

Migration assays were performed using Transwell (Falcon-Corning, Tewksbury, MA, USA; pore size, 8 μm) 24-well plates. Prior to performing the assay, the cells were pretreated on different SAM surfaces for 24 h, digested with trypsin and resuspended at a density of 5×10^4 cells in 150 μL of serum-free medium. The cells were then placed in the upper chamber, and 800 μL of the same medium containing 20% FBS was placed in the lower chamber. The plates were incubated for 24 h at 37°C in 5% CO_2. Next, the cells were fixed in 100% methanol for 30 min and then stained with 0.05% crystal violet in PBS for 30 min. The cells from the upper side of the filters were removed using cotton-tipped swabs, and the filters were washed with PBS. The cells from the underside of the filters were examined and counted using a microscope. Each group of pretreated cells was plated in triplicate in each experiment, and each experiment was repeated at least three times.[18-20]

2.6. Cell toxicity

Live/dead staining. Cell viability was assessed by live/dead staining with calcein AM and propidium iodide (PI). According to the manufacturer's protocol (Sigma, USA), 0.9 μL of calcein AM and 9 μL of PI solution were prepared in 3 mL of PBS. SPC-A-1 cells were seeded in 24-well plates at a concentration of 1×10^4 cells/mL at 37°C with 5% CO_2. The cells were allowed to attach to the SAMs for 24 h, washed with three times with PBS, then fixed with a freshly prepared stain for 30 min in the dark. The samples were then photographed using a fluorescence microscope (Olympus, BX51), and the cells dyed red and green were counted in five random fields.

Cell membrane integrity test (LDH release). Cells were cultured on different SAM-modified surfaces for 24 h, and lactate dehydrogenase (LDH) activity in the supernatants was measured spectrophotometrically by assaying reduced nicotinamide adenine dinucleotide oxidation at 340 nm during the LDH-catalyzed reduction of pyruvate to lactate.[21]

2.7. Cell apoptosis

SPC-A-1 cells were cultured for 24 h, washed three times with PBS, and then resuspended in 100 μL of RPMI 1640 with 1% FBS. The positive control was pretreated by co-culturing with cisplatin (10μmol/L) for 24h. The cells were stained in a 96-well microplate with Guava Nexin Reagent (Millipore, Billerica, MA, USA), a pre-made cocktail containing Annexin V-PE and 7-AAD in a final volume of 200 μL. After 20 min incubation at room temperature, the samples were analyzed using a Guava EasyCyte 5HT flow cytometer (Millipore, USA), and the data were analyzed using Guava Nexin Software v2. 2. 2.

2.8. Quantitative Real-time PCR (qRT-PCR)

PrimeScript RT Master Mix and SYBR Premix Ex Taq II (Takara) were used for cDNA synthesis and SYBR Green qRT-PCR according to the manufacturer's protocols, respectively. The qRT-PCR assays were performed by Rotor-Gene Q (Qiagen). All reactions were carried out in triplicate and the qRT-PCR results were analyzed using the Rotor-Gene Real-Time analysis software 6.0. Then relative gene expression of SPC-A-1 cells attached to the SAMs after incubation for 24 h was calculated using the $2^{-\Delta\Delta ct}$ method[60]. The cycling protocol was set as follows: 95°C for 10 min, followed by 45 cycles with each cycle made of 95°C for

15s, 60°C for 20s and 72°C for 20s. The primers used in the experiments were as follows:E-cadherin:F,5'-TGAAGGTG ACAGAGCCTCTGGAT-3' and R, 5'-TGGGTGAATTCGGGC TTGTT-3'; β-catenin: F, 5'-CCAGCGTGGACAATGGCTAC-3' and R, 5'-TGAGCTCGAGTCATTGCATAC-3'; GAPDH: F, 5'-GGAGCGAGATCCCTCCAAAAT-3' and R, 5'-GGCTGTTGTC ATACTTCTCATGG-3'.[22]

2.9. Statistical analysis

All statistical computations were performed with GraphPad Prism 5. The data were analyzed by ANOVA (analysis of variance) followed by Dunnett's multiple comparison test. The values were considered significantly different when $P<0.05$.

3. Results

3.1. Water contact angles of different model surfaces

The contact angles using water as the solvent for chemical group-modified coverslips are shown in Fig. 1. The surfaces ranged from hydrophobic for CH_3-terminated SAMs (103.4±3.2°) to hydrophilic for OH-SAMs (39.7±6.9°) and COOH-SAMs (50.1±2.3°). The surfaces of NH_2-SAMs and pristine gold (control group) had higher contact angle values of 68.9±4.5° and 77.3±0.5°, respectively. The contact angle for SH-SAMs was 87.8±0.5°, which is relatively hydrophobic.[23]

Fig. 1. Contact angle measurements using water as the solvent. The results are expressed as the means± SD of 5 independent experiments. SAMs terminated with the $-CH_3$ or -SH groups produced hydrophobic surfaces, while the $-NH_2$ and -COOH groups formed moderately wettable surfaces, and the -OH group created wettable surfaces.

3.2. Cell adhesion and spreading

After 24 h of incubation, SPC-A-1 cells exhibited various morphologies on different functional group-modified surfaces, as determined by SEM (Fig. 2). On the pristine gold surface (control), $-NH_2$, and -COOH-modified surfaces, a flat morphology and lamellipodia formations were observed around the cell bodies. On the -OH and -SH modified surfaces, the cells displayed a polygonal or spindle-like shape with filopodia at the leading edge. Whereas a more rounded or spindle-like shape and a smaller contact were found for the cells on the $-CH_3$ surface.

Fig. 2. SEM images of SPC-A-1 cells on SAM-modified surfaces after incubation for 24 h. (A) -CH3 surface; (B) -OH surface; (C) -COOH surface; (D) -NH2 surface; (E) -SH surface; (F) the pristine gold surface. The images were taken at ×300 and ×1500.

Focal adhesion analysis further confirmed the initial cell spreading difference modulated by different chemical functional groups. Representative images of cytoskeleton organization are presented in Fig.3.

Fig. 3. Fluorescent microscopy images displaying the cytoskeletal organization of SPC-A-1 cells on SAM-modified surfaces after incubation for 24 h. (A) $-CH_3$ surface; (B) -OH surface; (C) -COOH surface; (D) $-NH_2$ surface; (E) -SH surface; (F) the pristine gold surface. The images were taken at ×400.

DAPI staining was used to evaluate the initial adhesion of the SPC-A-1 cells. The number of adherent cells on different SAM-modified surfaces after 30, 60 and 90 min of incubation are shown in Fig. 4. Compared with the pristine gold surface, there were no differences in cell number among the $-CH_3$, -SH, -OH and -COOH groups at 30 min, whereas the cell number on the surface with the $-NH_2$ group was significantly increased ($p<0.001$). The cell numbers on the -COOH ($p<0.01$) and the $-NH_2$ surfaces ($p<0.001$) increased at 60 min. Although the $-CH_3$ and -SH groups showed no significant increase during the 90 min incubation, the cell numbers on the other groups increased over time, especially for the -COOH and $-NH_2$ groups. Interestingly, no obvious differences between the -OH and control groups were observed during the 90 min incubation. The adhesion numbers of SPC-A-1 cells followed the following trend: $-NH_2 \geqslant -COOH > -OH \geqslant Control >> -SH \approx -CH_3$.

Fig. 4. SPC-A-1 cells on SAM-modified surfaces measured by counting cells stained with DAPI using a fluorescence microscope after 30, 60 and 90 min of incubation. The control group refers to the pristine gold surface. The results represent the means± SD from 3 independent cultures and determinations. The symbols denote significant differences, as determined by two-way ANOVA, followed by the Bonferroni test. One symbol, $p<0.01$; two symbols, $p<0.001$. ∗ compared to the control at the same time. # compared to the substrates modified with the $-CH_3$ group at 90 min.

3. 3. Cell migration

When SPC-A-1 cells were cultured with different chemical group-modified surfaces for 24 h, significant differences in cell migration from the original aggregate were observed. Many cells migrated out from their original aggregate to the other side on -COOH and control surfaces. However, relatively few cells migrated on the $-CH_3$ and -SH substrates. Nevertheless, differences in behavior were apparent between the cells grown on the $-NH_2$ and -OH surfaces. Consequently, cell migration on these SAM-modified surfaces followed the following trend: $-COOH > -NH_2 \approx -OH >> -SH > -CH_3$ as shown in Fig. 5.

Fig. 5. The migration activity of each cell line after 24 h was determined in vitro by performing Transwell assays, (A) $-CH_3$ surface; (B) -OH surface; (C) -COOH surface; (D) $-NH_2$ surface; (E) -SH surface; (F) blank group. The results indicated a higher migration activity in the blank and -COOH groups. Cell migration was apparently prohibited by the $-CH_3$ and -SH groups.

3. 4. Cell toxicity

LDH is a cytoplasmic enzyme, and LDH activity is often associated with cell membrane damage and cell death.[21] The results of LDH activities are shown in Fig. 6. The $-CH_3$ and -SH groups showed significant toxicity toward SPC-A-1 cells compared with the pristine gold (Control) group ($p<0.05$).

Fig. 6. LDH activities in supernatants of SPC-A-1 cells cultured on different chemical groups after 24 h of incubation. Control group refered to the pristine gold surface. The results shown are the means± SD of three separate experiments performed in triplicate.∗ $p<0.05$ (one way ANOVA followed by Dunnett's multiple comparison test).

Cell toxicity was further confirmed by viability/cytotoxicity staining (Fig. 7). Numerous viable (green) cells were observed on all SAM-modified surfaces except those with the $-CH_3$ and –SH groups, on which relatively few non-viable (red) cells were found. These results confirmed that these two groups are toxic to SPC-A-1 cells.

Fig. 7. Fluorescence micrographs of live/dead dye-stained SPC-A-1 cells cultured on different chemical group- modified substrates for 24 h. (A) $-CH_3$ surface; (B) -OH surface; (C) -COOH surface; (D) $-NH_2$ surface; (E) -SH surface; (F) the pristine gold surface. The images were taken at ×100. The green cells represented viable cells and the red cells non-viable cells. $-CH_3$ and -SH exhibited cell toxicity toward SPC-A-1 cells.

3. 5. Cell apoptosis

To understand the possible mechanisms of the toxicity on different SAM-modified surfaces, SPC-A-1 cells were stained with PI and Annexin V-FITC and then analyzed by fluorescence-activated cell sorting (Fig. 8). CH_3-SAMs and SH-SAMs promoted SPC-A-1 cell necrosis with 17.2% and 15.3% necrotic cells, respectively, compared with the controls (4.0%). SH-SAMs also promoted apoptosis with 6.7% apoptotic cells compared with the controls (1. 0%). We found that the CH_3-SAMs (20.5%) and SH-SAMs (22.0%) induced almost the same apoptosis/necrosis rates as a 10μmol/L cisplatin-treated group (26.7%), and more information about the cisplatin's sensitive concentration to the SPC-A-1 cells can be get in supporting information (Fig. S2 and Fig. S3).

Fig. 8. Cell apoptosis assays with an Annexin V-FITC apoptosis detection kit. The SPC-A-1 cells were cultured on different SAM-modified surfaces for 24 h. The percentage of Annexin V (+) 7-AAD (+) cells revealed necrosis. The percentage of Annexin V (+) 7-AAD (-) cells revealed apoptosis. (A) -CH_3 surface; (B) -OH surface; (C) -COOH surface; (D) -NH_2 surface; (E) -SH surface; (F) the pristine gold surface; (G) the positive control group treated by cisplatin in 10μmol/L; (H) Blank group, SPC-A-1 cells without any treatment; (I) percent of cells undergoing apoptosis or necrosis(%) in different groups; * and $^{\#}$ denote significant differences (p<0.05) for apoptosis and necrosis, respectively, as determined by one-way ANOVA, followed by the Dunnett's Multiple Comparison Test compared to the pristine gold face.

3. 6. Expression of genes involed in metastatic behaviors

We then proceeded to investigate the effects of different SAMs on the expression of target genes involved in metastatic behaviors of SPC-A-1 cells, and to study the molecular mechanism. To this end, we measured the mRNA expression levels of E-cadherin and β-catenin using qRT-PCR analysis. The results showed that the relative expression of E-cadherin was significantly down regulated with the -CH_3, -OH, -NH_2 groups ($p < 0.01$), but significantly up regulated with -COOH ($p < 0.01$) and -SH groups ($p < 0.05$). The ratio of β-catenin was significantly down regulated in -OH ($p < 0.05$), -NH_2 groups, but those on the -COOH group showed a significant increase ($p < 0.01$). There was no significant change in β-catenin expression in the cells on the -CH_3 and -SH monolayers.

Fig. 9. Relative expression of E-cadherin and β-catenin genes in SPC-A-1 cells after incubation with different SAM-modified groups for 24h. In each case, the data was normalized to the expression level of GAPDH. Control group refers to the pristine gold surface. The relative expression levels of E-cadherin were significantly down regulated in -CH_3, -OH, -NH_2 groups, whereas the -COOH ($p < 0.01$) and -SH groups ($p < 0.05$) resulted in a significant increase. The ratio of β-catenin was significantly down regulated in -OH ($p < 0.05$), -NH_2 ($p < 0.01$) groups, but up regulated in -COOH groups ($p < 0.01$). All data represent the means ± standard deviation of three independent experiments. *: compared to the pristine gold surface. (one symbol, $p < 0.05$; two symbols, $p < 0.01$).

4. Discussion

Metastasis (from an initial primary tumor viaangiogenesis, intravasation, survival in the bloodstream, extravasation and metastatic growth) is an inefficient process, and few released cancer cells complete the entire course. Changes in adhesive characteristics and motility of cells have long been suspected to play an important role in mediating the spread of malignant neoplasms.[3, 7, 24, 25] We used the SAM model to explore the effect of chemical groups on SPC-A-1 cells *in vitro*.

First, cellular adhesion on biomaterial surfaces is a complex process that is affected by multiple factors. Nonspecific forces arise from the substrate's physicochemical characteristics, and specific forces can be presented as a result of receptor-ligand binding events between receptors on the cell surface and the physisorbed or chemisorbed proteins, peptides, and other bioactive factors on the material's surface.[26] Surface wettability has been shown to be an important factor in protein adhesion to biomaterial surfaces, and protein adhesion forces were found to increase with contact time, consistent with the surface-induced conformational changes in proteins.[27] Based on the morphology of single SPC-A-1 cells adhered onto different SAM-modified surfaces, the adhesion of SPC-A-1 cells changed in response to the surface chemistry (Fig. 2, Fig. 3). Fewer cells adhered onto the -CH_3 surface, and most exhibited a spindle shape; furthermore, the contact area was much smaller compared with the other groups. Conversely, SPC-A-1 cells on the -NH_2 and -COOH surfaces exhibited more spreading, which is consistent with previous studies.[14, 16, 26] Our results demonstrated that the hydrophobic CH_3-SAMs and SH-SAMs inhibit the pro-adhesion of SPC-A-1 cells, whereas the hydrophilic NH_2-SAMs and COOH-SAMs promote cell adhesion. However, the variations in cell adhesion and morphology observed for SPC-A-1 cells cannot be explained merely by the characteristics discussed above. For example, the cells on the -SH surfaces displayed a polygonal shape that was obviously different from the cells on the CH_3-SAMs, even though they both produced high contact angles. The adhesion number on the OH-SAMs was smaller than that on the NH_2-SAMs and COOH-SAMs, despite the higher contact angle. Thus, other characteristics including surface charge, surface energy and receptor-ligand binding should be considered.[28, 29]

Second, cell viability plays important role in the process of metastasis, which is invariably affected by the tumor microenvironment. Our results (Fig. 6, Fig. 7) demonstrated that the CH_3-SAMs and SH-SAMs exert cell toxicity toward SPC-A-1 cells, indeed, these functional groups may promote cell apoptosis.[30] Early apoptosis is also indicated by Annexin V-FITC-positivity and PI-negativity, and the results of the cell apoptosis assay supported the cell toxicity results described above.

Third, mobility is one of the primary events of the invasion-metastasis cascade.[31] The basic migratory cycle includes the extension of a protrusion, the formation of stable attachments near the leading edge of the protrusion, translocation of the cell body forward, the release of adhesions and retraction at the cell rear. Lamellipodia and filopodia play a key role in cell migration. Previous studies have reported a similar relationship between cytoskeletal assembly and cell migration, and increased vinculin expression has been shown to reduce cell motility.[24, 32-34] In our study, although SPC-A-1 cell lamellipodia were easily observed on the NH_2-SAMs and COOH-SAMs, lamellipodia were not found with the -CH_3-SAMs (Fig. 2). Furthermore, numerous actin stress fiber bundles anchored to the plasma membrane were observed on the -COOH surfaces (Fig. 3), whereas stress fiber formation was largely inhibited on the -CH_3 surfaces.

Finally, we found that SPC-A-1 cells exhibited high migration rates on the control and -COOH substrates yet lower migration rates on the -CH_3 and -SH substrates (Fig. 5). To explore the mechanism by which these different functional groups affect metastatic behaviors， we focused on the expression of E-cadherin and β-catenin in these cells. E-cadherin, a transmembrane cell adhesion molecule, is associated with three types of cytoplasmic proteins (alpha-catenin, beta-catenin and plakoglobin), and the formation of the cadherin-catenins adhesion complex is indispensable for tight cell-to-cell adhesion in adherence junctions. Loss of cadherin-mediated adhesion may promote cell migration and subsequent dissemination of lung cancer cells.[35-37] The qRT-PCR results (Fig. 9) showed a significant down-regulation of E-cadherin and β-catenin in cells on -NH_2 groups, and such reduced levels are associated with tumour invasion, metastasis, and unfavorable prognosis. Although the migratory ability of SPC-A-1 cells seemed to be prohibited on the CH_3-SAMs (Fig. 5), the ratio of E-cadherin was significantly down regulated on the -CH_3 group. Accordingly, the use of CH_3 group in lung cancer treatment should be reconsidered. However, E-cadherin was significantly up regulated on the SH-SAMs. Additional analyses are needed to explain the changes observed with the other chemical groups. To confirm these results, future studies will focus on alterations in larger set of genes and proteins.[2, 3, 830]

5. Conclusion

The data presented herein may be useful for a better understanding of cell–biomaterial interactions and for engineering new biomaterials or drugs. Our data indicate that SPC-A-1 cell behaviors, such as cell attachment efficiency, spreading behavior, actin stress fiber formation, and cell migration rates, are dependent on material surface chemistry. The -NH_2 and -COOH groups promoted adhesion and spreading, and the -OH group did not affect cell survival or mobility, in contrast, -CH_3 and -SH groups exhibited toxicity toward SPC-A-1 cells; Furthermore, the -SH group inhibited cell migration and increased metastasis-related gene expression. These results demonstrate that the -SH chemical group is potentially useful for designing novel lung cancer treatment strategies.

Acknowledgements

This study was supported by The National Natural Science Foundation of China (81271957, 81272507) and the Twelve five-year plan of military (cws11c268, bws11c065) and the Guangdong Key Laboratory of Orthopaedic Technology and Implant Materials in China ([2011]233-32). We also sincerely thank Jie Li, Xiaolan Wang and Qiaoting Hu for their assistance in the preparation of this manuscript.

Notes and references

[a] *Southern Medical University, Guangzhou, Guangdong， People's Republic of China*

[b]*Department of Orthopedics, Guangzhou General Hospital of Guangzhou Military Command, 111 Liuhua Road, Guangzhou 510010, China*

[c]*National engineering research center for tissue restoration and reconstruction, South China University of Technology, Guangzhou 510641, China*

**Author to whom correspondence should be addressed. Email: gzxiahong2@126.com*

[#]*These two authors contributed equally to this work.*

1. R. Siegel, J. Ma, Z. Zou and A. Jemal, *CA: a cancer journal for clinicians*, 2014, **64**, 9-29.
2. P. Mehlen and A. Puisieux, *Nature reviews. Cancer*, 2006, **6**, 449-458.
3. S. L. Wood, M. Pernemalm, P. A. Crosbie and A. D. Whetton, *Cancer treatment reviews*, 2014, **40**, 558-566.
4. J. Ferlay, H. R. Shin, F. Bray, D. Forman, C. Mathers and D. M. Parkin, *International journal of cancer. Journal international du cancer*, 2010, **127**, 2893-2917.
5. I. Sekine, H. Nokihara, N. Yamamoto, H. Kunitoh, Y. Ohe and T. Tamura, *Lung cancer (Amsterdam, Netherlands)*, 2009, **65**, 219-222.
6. S. Valastyan and R. A. Weinberg, *Cell*, 2011, **147**, 275-292.
7. A. F. Chambers, A. C. Groom and I. C. MacDonald, *Nature reviews. Cancer*, 2002, **2**, 563-572.
8. D. X. Nguyen, P. D. Bos and J. Massague, *Nature reviews. Cancer*, 2009, **9**, 274-284.
9. M. Mrksich, *Acta biomaterialia*, 2009, **5**, 832-841.
10. M. Mrksich and G. M. Whitesides, *Annual review of biophysics and biomolecular structure*, 1996, **25**, 55-78.
11. J. M. Curran, R. Chen and J. A. Hunt, *Biomaterials*, 2005, **26**, 7057-7067.
12. Y. J. Ren, H. Zhang, H. Huang, X. M. Wang, Z. Y. Zhou, F. Z. Cui and Y. H. An, *Biomaterials*, 2009, **30**, 1036-1044.
13. C. A. Scotchford, C. P. Gilmore, E. Cooper, G. J. Leggett and S. Downes, *Journal of biomedical materials research*, 2002, **59**, 84-99.
14. X.-L. Yu, S.-J. Xu, J.-D. Shao, C. Du, S.-F. Chen, B. Zhang, Y.-X. Wang and X.-M. Wang, *Surface and Coatings Technology*, 2013, **228**, S48-S54.
15. P. Filippini, G. Rainaldi, A. Ferrante, B. Mecheri, G. Gabrielli, M. Bombace, P. L. Indovina and M. T. Santini, *Journal of biomedical materials research*, 2001, **55**, 338-349.
16. H. Yan, S. Zhang, J. He, Y. Yin, X. Wang, X. Chen, F. Cui, Y. Li, Y. Nie and W. Tian, *Biomedical materials*, 2013, **8**, 035008.
17. P. Jal, S. Patel and B. Mishra, *Talanta*, 2004, **62**, 1005-1028.
18. C. H. Tang and M. E. Lu, *The Prostate*, 2009, **69**, 1781-1789.
19. I. Saiki, J. Murata, K. Watanabe, H. Fujii, F. Abe and I. Azuma, *Japanese journal of cancer research : Gann*, 1989, **80**, 873-878.
20. C. Y. Huang, Y. C. Fong, C. Y. Lee, M. Y. Chen, H. C. Tsai, H. C. Hsu and C. H. Tang, *Biochemical pharmacology*, 2009, **77**, 794-803.
21. G. Haslam, D. Wyatt and P. A. Kitos, *Cytotechnology*, 2000, **32**, 63-75.
22. M. Li, Y. Zhu, H. Zhang, L. Li, P. He, H. Xia, Y. Zhang and C. Mao, *Scientific reports*, 2014, **4**, 7380.
23. S. Jo and K. Park, *Biomaterials*, 2000, **21**, 605-616.
24. J. B. McCarthy, M. L. Basara, S. L. Palm, D. F. Sas and L. T. Furcht, *Cancer metastasis reviews*, 1985, **4**, 125-152.
25. P. A. Netland and B. R. Zetter, *The Journal of cell biology*, 1985, **101**, 720-724.
26. M. H. Lee, D. A. Brass, R. Morris, R. J. Composto and P. Ducheyne, *Biomaterials*, 2005, **26**, 1721-1730.
27. L.-C. Xu and C. A. Siedlecki, *Biomaterials*, 2007, **28**, 3273-3283.
28. M. P. Van Damme, J. Tiglias, N. Nemat and B. N. Preston, *Analytical biochemistry*, 1994, **223**, 62-70.
29. S. A. Makohliso, R. F. Valentini and P. Aebischer, *Journal of biomedical materials research*, 1993, **27**, 1075-1085.
30. D. E. Ingber, *Seminars in cancer biology*, 2008, **18**, 356-364.
31. S. Y. Lee, S. Voronov, K. Letinic, A. C. Nairn, G. Di Paolo and P. De Camilli, *The Journal of cell biology*, 2005, **168**, 789-799.
32. D. J. Webb, J. T. Parsons and A. F. Horwitz, *Nat Cell Biol*, 2002, **4**, E97-100.
33. A. J. Ridley, M. A. Schwartz, K. Burridge, R. A. Firtel, M. H. Ginsberg, G. Borisy, J. T. Parsons and A. R. Horwitz, *Science (New York, N.Y.)*, 2003, **302**, 1704-1709.
34. J. L. Rodriguez Fernandez, B. Geiger, D. Salomon and A. Ben-Ze'ev, *Cell motility and the cytoskeleton*, 1992, **22**, 127-134.

35. H. Shibanuma, T. Hirano, K. Tsuji, Q. Wu, B. Shrestha, C. Konaka, Y. Ebihara and H. Kato, *Lung cancer (Amsterdam, Netherlands)*, 1998, **22**, 85-95.
36. J. M. Retera, M. P. Leers, M. A. Sulzer and P. H. Theunissen, *Journal of clinical pathology*, 1998, **51**, 891-894.
37. R. M. Bremnes, R. Veve, F. R. Hirsch and W. A. Franklin, *Lung cancer (Amsterdam, Netherlands)*, 2002, **36**, 115-124.

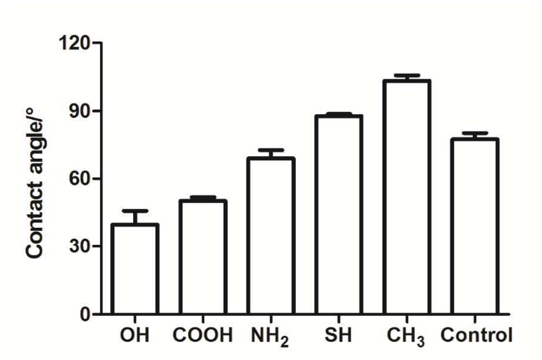

Fig. 1. Contact angle measurements using water as the solvent. The results are expressed as the means±SD of 5 independent experiments. SAMs terminated with the -CH_3 or -SH groups produced hydrophobic surfaces, while the -NH_2 and -COOH groups formed moderately wettable surfaces, and the -OH group created wettable surfaces.

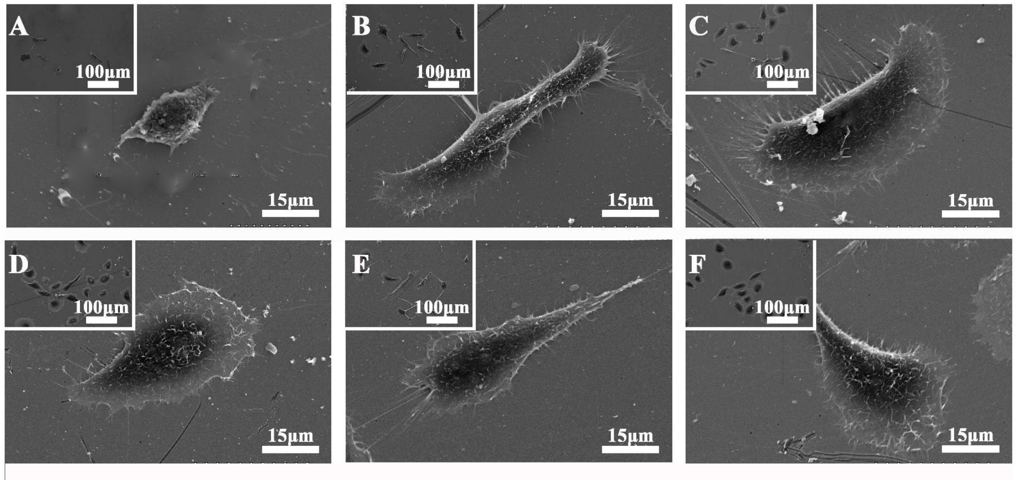

Fig. 2. SEM images of SPC-A-1 cells on SAM-modified surfaces after incubation for 24 h. (A) -CH3 surface; (B) -OH surface; (C) -COOH surface; (D) -NH2 surface; (E) -SH surface; (F) the pristine gold surface. The images were taken at ×300 and ×1500.

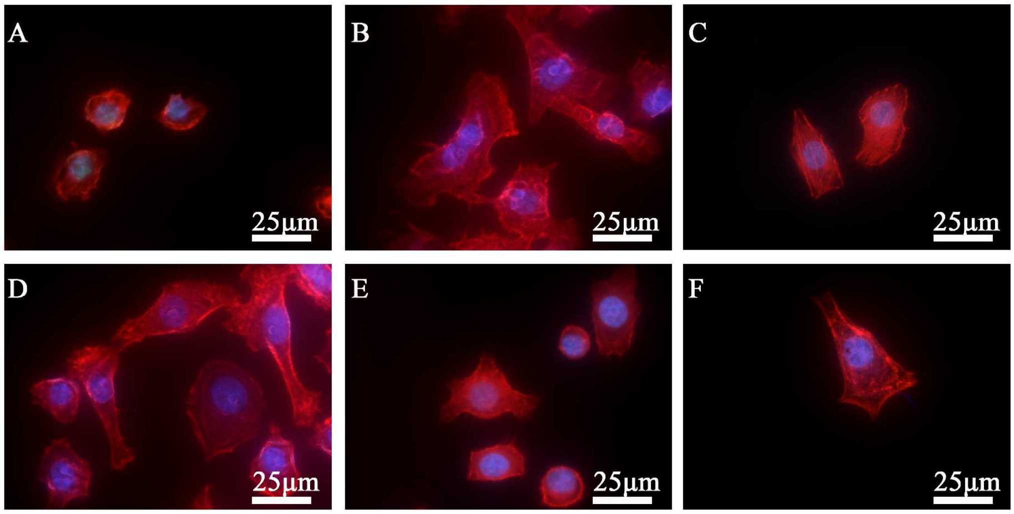

Fig. 3. Fluorescent microscopy images displaying the cytoskeletal organization of SPC-A-1 cells on SAM-modified surfaces after incubation for 24 h. (A) -CH_3 surface; (B) -OH surface; (C) -COOH surface; (D) -NH_2 surface; (E) -SH surface; (F) the pristine gold surface. The images were taken at ×400.

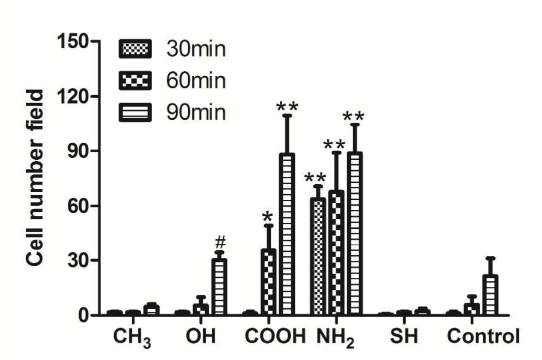

Fig. 4. SPC-A-1 cells on SAM-modified surfaces measured by counting cells stained with DAPI with a fluorescence microscope after 30, 60 and 90 min of incubation. The Control group refered to the pristine gold surface. The results represent the means± SD from 3 independent cultures and determinations. The symbols denote significant differences, as determined by two-way ANOVA, followed by the Bonferroni test. One symbol, $p<0.01$; two symbols, $p<0.001$. ∗ compared to the control at the same time. # compared to the substrates modified with the $-CH_3$ group at 90 min.

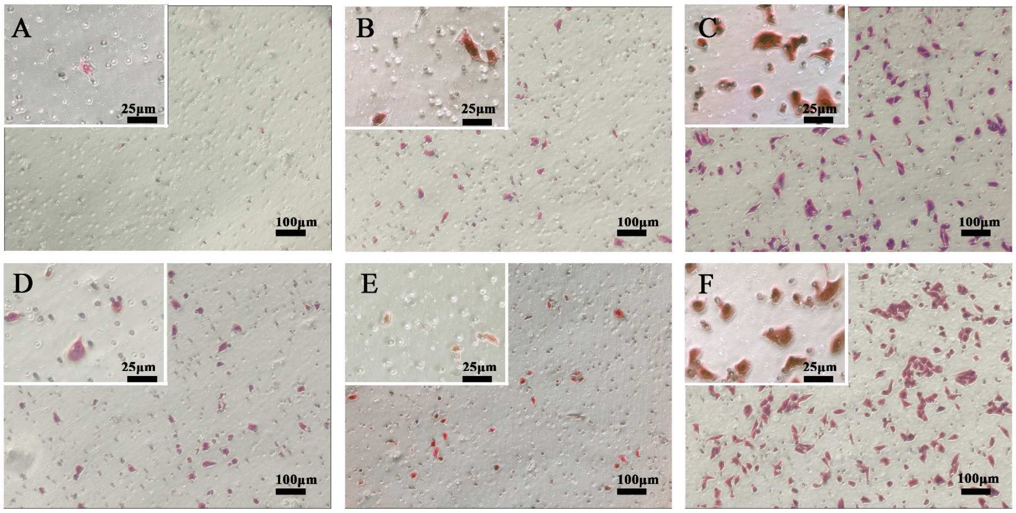

Fig. 5. The migration activity of each cell line after 24 h was determined in vitro by performing Transwell assays, (A) -CH_3 surface; (B) -OH surface; (C) -COOH surface; (D) -NH_2 surface; (E) -SH surface; (F) blank group. The results indicated a higher migration activity in the blank and -COOH groups. Cell migration was apparently prohibited by the -CH_3 and -SH groups. The images were taken at ×100 and ×200.

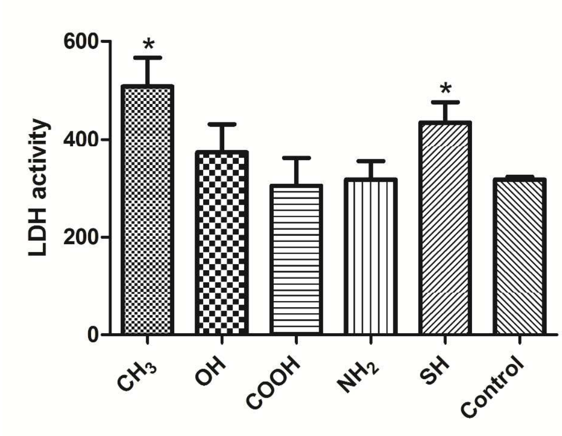

Fig. 6. LDH activities in supernatants of SPC-A-1 cells cultured on different chemical groups after 24 h of incubation. Control group refered to the pristine gold surface. Results shown were the mean± SD of three separate experiments performed in triplicate.∗ $p<0.05$ (one way ANOVA followed by Dunnett's multiple comparison test).

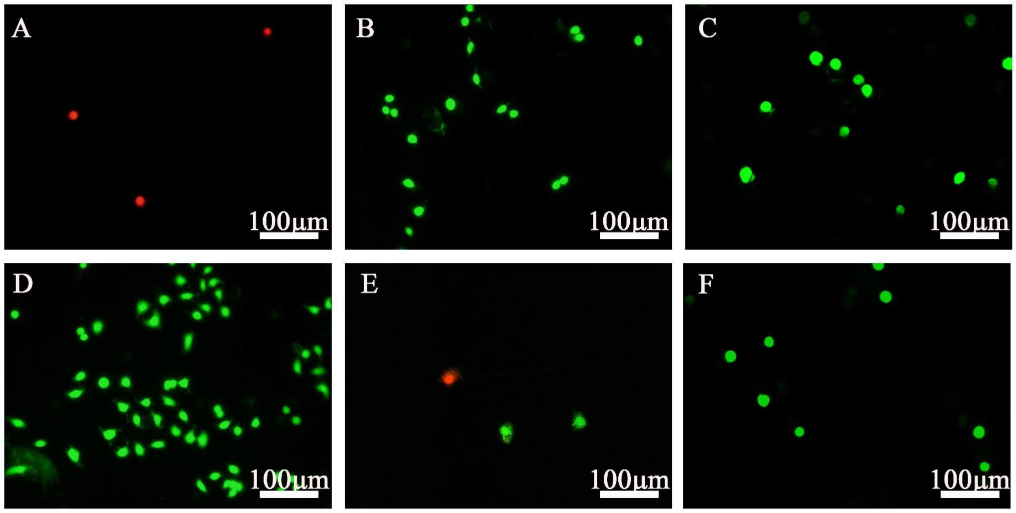

Fig. 7. Fluorescence micrographs of live/dead dye-stained SPC-A-1 cells cultured on different chemical group- modified substrates for 24 h. (A) -CH_3 surface; (B) -OH surface; (C) -COOH surface; (D) -NH_2 surface; (E) -SH surface; (F) the pristine gold surface. The images were taken at ×100. The green cells represented viable cells and the red cells were non-viable cells. -CH_3 and -SH exhibited cell toxicity toward SPC-A-1 cells.

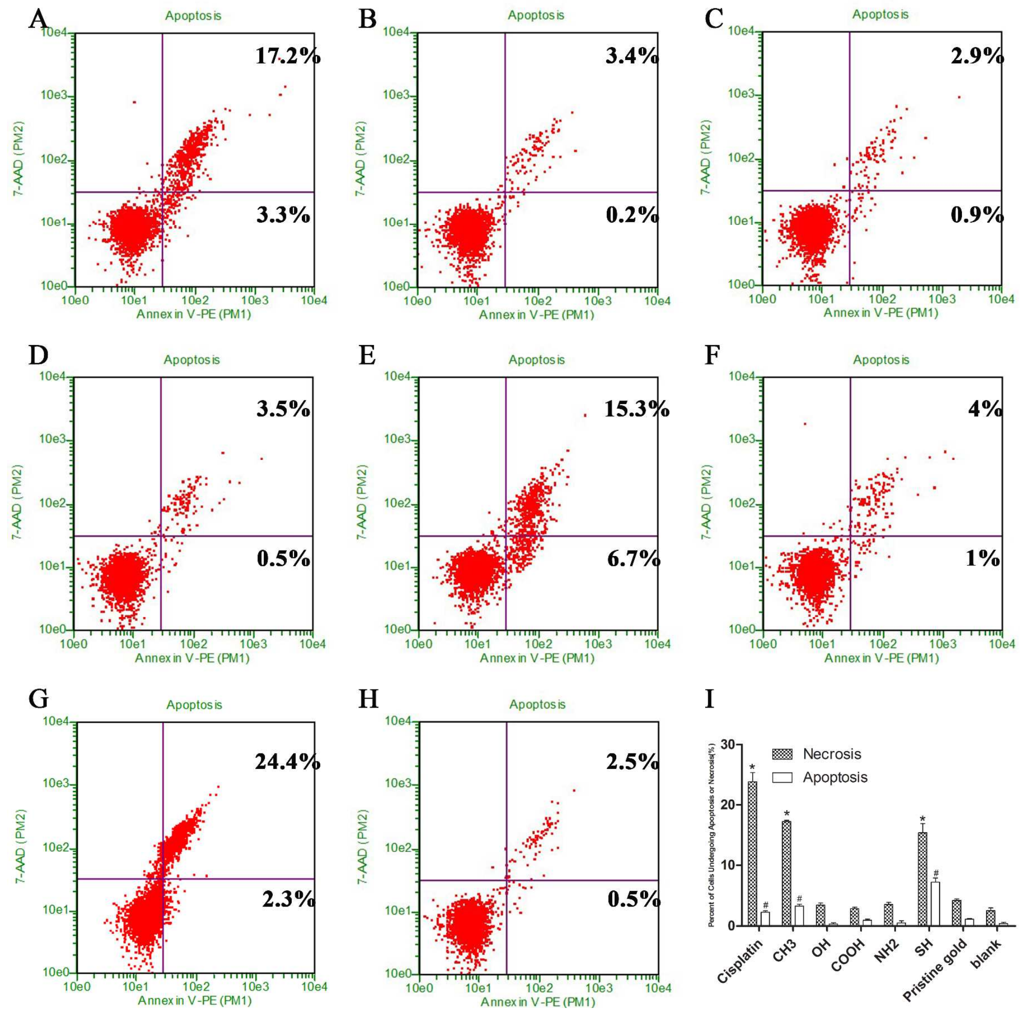

Fig. 8. Cell apoptosis assays with an Annexin V-FITC apoptosis detection kit. The SPC-A-1 cells were cultured on different SAM-modified surfaces for 24 h. The percentage of Annexin V (+) 7-AAD (+) cells revealed necrosis. The percentage of Annexin V (+) 7-AAD (-) cells revealed apoptosis. (A) $-CH_3$ surface; (B) -OH surface; (C) -COOH surface; (D) $-NH_2$ surface; (E) -SH surface; (F) the pristine gold surface; (G) the positive control group treated by cisplatin in 10μmol/L; (H) Blank group, SPC-A-1 cells without any treatment; (I) percent of cells undergoing apoptosis or necrosis(%) in different groups; * and # denote significant differences ($p<0.05$) for apoptosis and necrosis, respectively, as determined by one-way ANOVA, followed by the Dunnett's multiple comparison test compared to the pristine gold face.

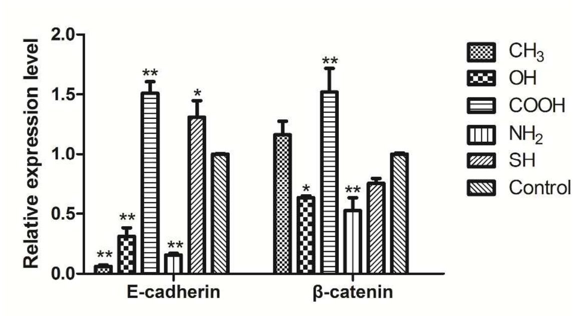

Fig. 9. Relative expression of E-cadherin and β-catenin genes in SPC-A-1s after incubation with different SAM-modified groups for 24h. In each case, the data was normalized to the expression level of GAPDH. Control group refers to the pristine gold surface. Relative expression levels of E-cadherin were significantly down regulated in $-CH_3$, -OH, $-NH_2$ groups, while -COOH ($p < 0.01$) and -SH groups ($p < 0.05$) showed significant increase. The ratios of β-catenin were significantly down regulated in -OH ($p < 0.05$), $-NH_2$ ($p < 0.01$) groups, but up regulated in -COOH groups ($p < 0.01$). All data represent the mean ± standard deviation of three independent experiments. *: compared to the pristine gold surface. (One symbol, $p < 0.05$; two symbols, $p < 0.01$).